J. Membrane Biol. 208, 229–240 (2005)
DOI: 10.1007/s00232-005-0830-z

The Journal of
Membrane
Biology

BK_{Ca} Channels Activating at Resting Potential without Calcium in LNCaP Prostate Cancer Cells

G. Gessner[1], K. Schönherr[1], M. Soom[1], A. Hansel[1], M. Asim[2], A. Baniahmad[2], C. Derst[3], T. Hoshi[4], S.H. Heinemann[1]

[1]Institute of Molecular Cell Biology, Molecular and Cellular Biophysics, Friedrich Schiller University Jena, Germany
[2]Institute of Human Genetics and Anthropology, Molecular Genetics, Friedrich Schiller University Jena, Germany
[3]Center for Anatomy, Electronmicroscopy and Molecular Neuroanatomy, Charité Berlin, Germany
[4]Department of Physiology, University of Pennsylvania, Philadelphia, PA, USA

Received: 29 July 2005/Revised: 15 December 2005

Abstract. Large-conductance Ca^{2+}-dependent K^+ (BK_{Ca}) channels are activated by intracellular Ca^{2+} and membrane depolarization in an allosteric manner. We investigated the pharmacological and biophysical characteristics of a BK_{Ca}-type K^+ channel in androgen-dependent LNCaP (lymph node carcinoma of the prostate) cells with novel functional properties, here termed BK_L. K^+ selectivity, high conductance, activation by Mg^{2+} or NS1619, and inhibition by paxilline and penitrem A largely resembled the properties of recombinant BK_{Ca} channels. However, unlike conventional BK_{Ca} channels, BK_L channels activated in the absence of free cytosolic Ca^{2+} at physiological membrane potentials; the half-maximal activation voltage was shifted by about −100 mV compared with BK_{Ca} channels. Half-maximal Ca^{2+}-dependent activation was observed at 0.4 μM for BK_L (at −20 mV) and at 4.1 μM for BK_{Ca} channels (at +50 mV). Heterologous expression of hSlo1 in LNCaP cells increased the BK_L conductance. Expression of *hSlo-β1* in LNCaP cells shifted voltage-dependent activation to values between that of BK_L and BK_{Ca} channels and reduced the slope of the P_{open} (open probability)-voltage curve. We propose that LNCaP cells harbor a so far unknown type of BK_{Ca} subunit, which is responsible for the BK_L phenotype in a dominant manner. BK_L-like channels are also expressed in the human breast cancer cell line T47D. In addition, functional expression of BK_L in LNCaP cells is regulated by serum-derived factors, however not by androgens.

Correspondence to: S.H. Heinemann; email: Stefan.H.Heinemann@uni-jena.de

Key words: BK_{Ca} channel — Ca^{2+}-activated K^+ channel — Patch clamp — K^+ channel blocker — K^+ channel opener — β subunit

Introduction

Depolarization and free cytosolic calcium ($[Ca^{2+}]_{in}$) synergistically activate large-conductance Ca^{2+}-activated potassium (BK_{Ca}) channels (Kaczorowski et al., 1996). In a functional BK_{Ca} channel complex, each of the four (Shen et al., 1994) α (Slo1) subunits likely contains six major segments (S1 to S6) plus an additional N-terminal S0 segment, thought to interact with an accessory β subunit, and a large cytoplasmic C-terminus important for Ca^{2+} binding (Meera et al., 1997; Xia et al., 2002). A high-affinity (< 10 μM $[Ca^{2+}]_{in}$) and a low-affinity (>100 μM $[Ca^{2+}]_{in}$ or $[Mg^{2+}]_{in}$) binding site located in the C-terminus enable BK_{Ca} channels to respond to changes in $[Ca^{2+}]_{in}$ ranging from 500 nM to 50 mM (Xia et al., 2002). Even in the absence of Ca^{2+}, depolarization alone can open BK_{Ca} channels but the half-maximal activation voltage ($V_{0.5}$) under such a condition is typically far outside the physiological range (> +100 mV) (Horrigan et al., 1999; Meera et al., 1996). Activation of typical BK_{Ca} channels at physiological voltages requires micromolar levels of $[Ca^{2+}]_{in}$.

In excitable cells, activation of BK_{Ca} channels facilitates hyperpolarization and thereby reduces Ca^{2+} entry through voltage-gated channels. By providing an inhibitory influence on cellular excitability, BK_{Ca} channels regulate the shape of action potentials (Shao et al., 1999), neurotransmitter release (Kaczorowski et al., 1996), smooth muscle contraction (Brenner et al., 2000), and electrical tuning of hair cells

(Ramanathan et al., 1999). To fulfill this broad spectrum of functions, properties of BK_{Ca} channels are remarkably diverse and at least three mechanisms contribute to this functional diversity. First, alternative splicing of the underlying single gene *slo1* or *KCNMA1*, regulated at least in part by steroid hormones (Xie & McCobb, 1998; Lai & McCobb, 2002), creates multiple pore-forming α subunit isoforms (Tseng-Crank et al., 1994). Second, auxiliary β subunits encoded by four different genes (*slo*β*1*–β*4* or *KCNMB1–4*) coassemble with α subunits to further increase the diversity (Orio et al., 2002). Third, post-translational modifications of BK_{Ca} α and/or β subunits, such as phosphorylation and oxidation (reviewed in Weiger et al., 2002), markedly alter the functional properties of BK_{Ca} channel complexes.

BK_{Ca} channels are found in virtually all cell types, including some cancer cells such as human glioma (Liu et al., 2002) and astrocytoma (Basrai et al., 2002) where they may play critical roles in control of cell proliferation and malignancy grade. In lymph node carcinoma of the prostate (LNCaP) cells (Horoszewicz et al., 1983), which serve as a model system in which to study androgen-dependent proliferation and apoptosis of cancer cells, the existence of BK_{Ca} channels has been also speculated but not unequivocally demonstrated: Gutiérrez et al. (1999) inferred that hyperpolarization caused by an apoptosis inducer was mediated by activation of BK_{Ca} channels. The postulated BK_{Ca} channel should be clearly distinguishable from the Ca^{2+}-inhibited K^+ channel described in LNCaP cells (Skryma et al., 1999). This voltage-dependent 78-pS K^+ channel, accounting for most of the whole-cell K^+ current (<600 pA at 40 mV), was half-maximally inhibited by 0.5 μM $[Ca^{2+}]_{in}$ but insensitive to charybdotoxin (ChTx) and iberiotoxin (IbTx), two toxins that normally inhibit BK_{Ca} channels (Dworetzky et al., 1996).

The aim of this study was to demonstrate that LNCaP cells express BK_{Ca} channels and to examine whether their functional features are altered by androgens. We found a novel type of BK_{Ca} channel (termed BK_L) with an unusual voltage and $[Ca^{2+}]_{in}$ dependence: activation at physiological voltages even in the absence of Ca^{2+}. Similar BK_{Ca} channels were also present in T47D breast cancer cells. Thus we conclude that these BK_{Ca} channels with the aforementioned unusual activation properties are physiologically relevant for functions not only in prostate cancer cells.

Materials and Methods

Cell Culture and Molecular Biology

LNCaP cells (DSMZ) and T47D cells (ATCC) were grown at 37°C in a humidified atmosphere with 5% CO_2 in RPMI 1640 medium (Invitrogen, Karlsruhe, Germany) supplemented with L-glutamine and 10% fetal calf serum (FCS). Cells were seeded on gelatin-coated 35-mn plates in culture medium 2–5 days before electrophysiological measurements. HEK293 cells (DSMZ) were maintained in DMEM / F-12 medium (1:1; Invitrogen) supplemented with 10% FCS. A second LNCaP cell line (ATCC) was cultured in RPMI 1640 medium supplemented with L-glutamine, sodium pyruvate, 10% FCS, 1% penicillin, and 1% streptomycin (Sigma, Taufkirchen, Germany). Charcoal-treated serum was generated by incubating 500 ml FCS with activated charcoal (30 g; Sigma) for 4 h at 4°C, followed by centrifugation and sterile filtration. C4-2 cells (kindly provided by G. Thalmann) were maintained in 10% FCS-containing T-medium (Zhau et al., 1996). All other cell lines were maintained according to the distributor's instructions (DSMZ). Cells were used within passage numbers 3 to 20. R1881 (methyltrienolone) was a gift from Zeneca Pharmaceuticals (Wilmington, DE). Casodex was obtained from Perkin Elmer (Rodgau, Germany).

The Polyfect and Superfect transfection kits (Qiagen, Hilden, Germany) were used for transient transfection. *hKCNMA1* (hSlo1, U11058) was subcloned into pCI-neo (Promega, Mannheim, Germany). *hKCNMB1* (*hSlo*-β*1*) was amplified from a mixed brain and heart cDNA (Clontech, Heidelberg, Germany) and cloned into pcDNA3 (Invitrogen). An EGFP expression plasmid (pEGFPN1, Clontech) was co-transfected (20% of DNA) allowing identification of transfected, fluorescent cells. mRNA from $\sim 5 \times 10^6$ LNCaP cells, isolated with the OligoTex Direct mRNA Kit (Qiagen), was used for RT-PCR with the Titan One Tube RT-PCR Kit (Roche, Mannheim, Germany). Gene-specific primers (Jena Bioscience, Jena, Germany and MWG Biotech, Munich, Germany) were designed according to the published human sequences. PCR fragments were subcloned into pGEM-T (Promega) and sequenced using thermosequenase (Fermentas, St. Leon-Rot, Germany) and the Li-Cor 4000 automated sequencer (MWG Biotech).

Electrophysiological Recordings

Electrophysiological data were obtained with an EPC-9 patch-clamp amplifier (HEKA Elektronik, Lambrecht, Germany). Data acquisition and analysis were controlled with Pulse + PulseFit, PatchMaster (HEKA), and IgorPro (WaveMetrics. Lake Oswego, OR) software. Patch pipettes fabricated from borosilicate glass had initial resistances of 1–2 and 5–15 MΩ for whole-cell and single-channel experiments, respectively. The internal solutions contained (in mM): 140 KCl, 2 $MgCl_2$, 10 HEPES, pH 7.4. Free intracellular calcium concentrations ($[Ca^{2+}]_{in}$) were adjusted by adding $CaCl_2$ to either 10 mM EGTA (1–300 nM $[Ca^{2+}]_{in}$ with or without 2 mM $[Mg^{2+}]$) or 10 mM HEDTA (0.3–100 μM $[Ca^{2+}]_{in}$) buffered solutions, as calculated by Patcher's Power Tools (http: //www.mpibpc.gwdg.de/abteilungen/140/software/), considering Mg^{2+} and ATP concentrations (if added). The external solution contained (in mM): 135 NaCl, 5 KCl, 2 $MgCl_2$, 2 $CaCl_2$, 10 HEPES, pH 7.4. For measurements under bi-ionic conditions (likewise in symmetrical (140 mM) K^+) NaCl and KCl were replaced by the chloride salt of the monovalent species under consideration. In the whole-cell configuration, currents were measured with access resistances below 4 MΩ. Series resistance compensation was applied up to 90%.

To measure the voltage dependence, 100-ms depolarization pulses to various voltages were applied. Instantaneous tail-current amplitudes (I_{inst}) were plotted against voltage and fitted with a Boltzmann function:

$$I_{inst} = I_{inst,max}/(1 + \exp((V_{0.5} - V)/k_a)) \quad (1)$$

where $I_{inst,max}$ is the maximum instantaneous current, $V_{0.5}$ is the voltage for half-maximal activation, and k_a is a factor characterizing the steepness of the voltage dependence. Alternatively, voltage dependence was quantified by fitting steady-state

currents with a combined Boltzmann / GHK constant-field equation:

$$I(V) = G_{max}(1+\exp(V_{0.5}-V)/k_a) \\ (1-\exp((V_{rev}-V)/25mV))/(1-\exp(-V/25mV)) \quad (2)$$

where G_{max} is the maximum conductance, V_{rev} is the reversal potential, and $V_{0.5}$ and k_a have the same meaning as in Eq. (1). Reversal potentials, measured under bi-ionic conditions, were used to calculate permeability coefficients.

All chemicals used were of high grade, obtained from Sigma, except iberiotoxin, paxilline, and penitrem A were purchased from Alomone (Jerusalem, Israel). Blockers were applied with an application pipette and the time course of block was monitored by repetitive stimulation. Inhibition was analyzed by measuring the steady-state current, plotting the fractional current block against the blocker concentration, and fitting a Hill equation to these data:

$$I/I_{control} = 1/\left(1+\left([blocker]/IC_{50}\right)^h\right) \quad (3)$$

where IC_{50} represents the inhibitor concentration yielding 50% block and h is the Hill coefficient.

Single-channel analysis was performed on continuous current records of patches containing 1–2 channels. Records were low-pass filtered at 2 kHz and sampled at 10 kHz. Fits with double Gaussian functions to all-points amplitude histograms were used to estimate the unitary current amplitudes (i). Single-channel conductances were determined from the linear i / V slope between −30 and + 80 mV. Open probabilities (P_{open}) were calculated from the integrated peak areas with a 50% threshold value between mean open and closed state currents. The maximal number of simultaneously open channels at high voltage (with a $P_{open} > 50\%$) was defined as number of channels per patch. To assay the voltage dependence, P_{open} / V data were fitted with a Boltzmann function (Eq. 1) with I_{inst} replaced by P_{open} data.

Calcium dependence was assayed by plotting P_{open} at constant voltage against $[Ca^{2+}]_{in}$ and fitting a modified Hill function to the data:

$$P_{open} = P_{open,min} + \left(P_{open,max} - P_{open,min}\right)/\left(1+\left([Ca^{2+}]/EC_{50}\right)^h\right) \quad (4)$$

with the half-maximally activating concentration EC_{50} and the Hill coefficient h.

All data are given as mean ± SEM (n), where n is the number of independent experiments. Statistical comparisons were made using a two-sided Student's t-test. Statistical significance was assumed at $P < 0.05$.

Results

Potassium Channels in LNCaP Cells with and without Ca^{2+}

LNCaP cells are reported to contain Ca^{2+}-activated (Gutiérrez et al., 1999) as well as Ca^{2+}-inhibited (Skryma et al., 1999) voltage-dependent K^+ (K_v) channels. We recorded robust voltage-dependent whole-cell currents from LNCaP cells with 0 and 3 μM free $[Ca^{2+}]_{in}$ (Fig. 1*A, B*). At 100 mV, the currents were often greater than 20 nA and the average current densities were 1.40 ± 0.15 nA / pF ($n = 28$) and 1.65 ± 0.31 nA / pF ($n = 35$) in 0 and 3 μM $[Ca^{2+}]_{in}$, respectively. While the average current densities were not different in 0 and 3 μM $[Ca^{2+}]_{in}$, our density estimates were ~20-fold greater than observed by Skryma et al. (1999).

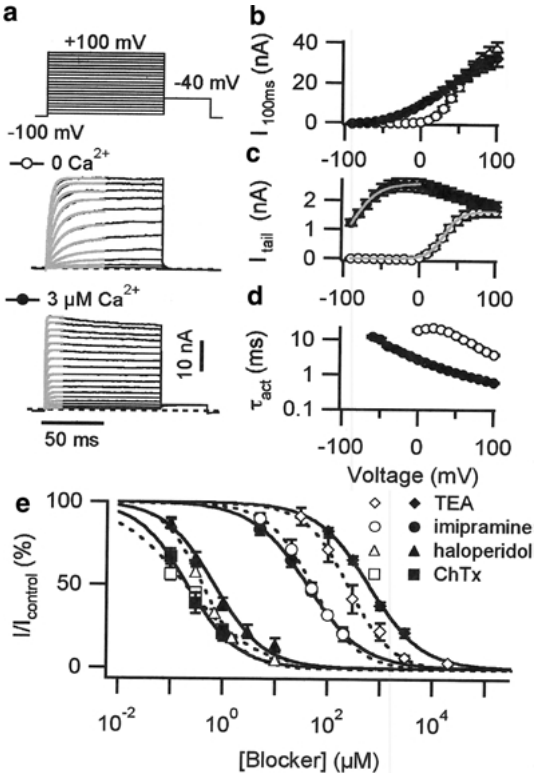

Fig. 1. Ca^{2+}-sensitive whole-cell currents in LNCaP cells. (*A*) Representative whole-cell currents of two different LNCaP cells with 0 or 3 μM $[Ca^{2+}]_{in}$. (*B*) Steady-state current amplitudes were averaged for 28 and 35 cells, respectively, and plotted against voltage. (*C*) Tail currents were measured immediately following the voltage step to −40 mV. Mean tail currents were plotted against the voltage and fitted with a Boltzmann function (*line*). (*D*) Activation time constants in 0 and 3 μM $[Ca^{2+}]_{in}$, as obtained by single exponential fits (superimposed in *A*) at different voltages. (*E*) Concentration-response curves of whole-cell conductances in 0 (*empty symbols*) or 3 μM (*filled symbols*) free $[Ca^{2+}]_{in}$. Steady-state currents were normalized to the control current before blocker application and averaged for 4–6 cells. Solid lines are best fits with a Hill function (Eq. 3).

Voltage dependence of the whole-cell currents depended on $[Ca^{2+}]_{in}$. Increasing $[Ca^{2+}]_{in}$ from 0 to 3 μM changed the mean $V_{0.5}$ value estimated from the tail currents from +32.9 ± 1.3 mV to −89.7 ± 1.5 mV ($P < 0.001$), a −120 mV shift to the negative direction. The same change in $[Ca^{2+}]_{in}$ also increased the slope factor k_a from 12.1 ± 0.5 mV to 16.9 ± 0.6 mV ($P < 0.001$). The activation kinetics, well characterized by a single exponential, was also markedly dependent on $[Ca^{2+}]_{in}$, being faster in 3 μM $[Ca^{2+}]_{in}$ (Fig. 1*A, D*).

The channels underlying the whole-cell currents were highly selective for K^+. Under bi-ionic conditions (140 mM K^+ inside), inward tail currents at −120 mV were detected only with (140 mM) K^+ or

Rb^+ (P_K/P_{Rb} = 1.2), but with Na^+, Cs^+, or Li^+ in the external solution. The permeability coefficient for K^+ over Na^+, Cs^+, and Li^+ was estimated to be greater than 115, according to their corresponding V_{rev} values of < -120 mV.

Activation by depolarization, high K^+ selectivity and a strong left-shift in $V_{0.5}$ together with faster activation with an increase in $[Ca^{2+}]_{in}$ are typical features of BK_{Ca} channels (Kaczorowski et al., 1996). However, conventional BK_{Ca} channels should exhibit almost no activity at +50 mV in 0 $[Ca^{2+}]_{in}$ and even in 3 μM $[Ca^{2+}]_{in}$ typical $V_{0.5}$ values are above 0 mV (Meera et al., 1996). Hence, if a single type of channel predominated the LNCaP whole-cell conductance, this would be either a novel K_v channel or a BK_{Ca} channel with unprecedented features. Alternatively, two channel types, exclusively active in either 0 or 3 μM $[Ca^{2+}]_{in}$ could be present in LNCaP cells.

To distinguish between the above possibilities, we analyzed channel inhibition by increasing concentrations of various drugs: tetraethylammonium (TEA), imipramine, haloperidol, and ChTx (Fig. 1*E*). The effects of these compounds were monitored by 100-ms depolarizations to +100 mV, repeated every 3 s. The inhibitory effects of imipramine, TEA, and haloperidol equilibrated within 90 s of drug application. However, the onset of block by ChTx was extremely slow and the results obtained 5 min after application may not represent full equilibrium, thus underestimating the true inhibitory efficacy. In 0 $[Ca^{2+}]_{in}$, fits with the Hill equation (Eq. 3) yielded IC_{50} values of 235 μM, 49.2 μM, 399 nM, and 192 nM for TEA, imipramine, haloperidol, and ChTx, respectively. In 3 μM $[Ca^{2+}]_{in}$, the corresponding IC_{50} values were 610 μM, 41.1 μM, 684 nM, and 207 nM. Hill coefficients were always near unity. Taking into account a state dependence of block by TEA and haloperidol (*not shown*), the whole-cell currents in 0 and 3 μM $[Ca^{2+}]_{in}$ displayed indistinguishable blocker sensitivities, suggesting that the currents were mediated by a single channel type. To distinguish between K_v and BK_{Ca} type channels as potential molecular correlates, we tested the effects of BK_{Ca}-specific blockers. In 0 $[Ca^{2+}]_{in}$, IbTx slowly blocked the whole-cell currents with an estimated IC_{50} of 120 nM. Onset of block by paxilline and penitrem A was faster and the IC_{50} values were 16.4 nM and 11.0 nM, respectively. The high inhibitory efficacies of these BK_{Ca} blockers strongly implicate that a class of BK_{Ca} channels with a novel voltage dependence underlies the whole-cell current in LNCaP cells.

Single-Channel Analysis

We performed outside-out (OO) single-channel recordings with 5 mM K^+ outside and 140 mM K^+ inside (Fig. 2*A*) to analyze this putative BK_{Ca}-type channel. Calculated single-channel conductance (γ) values were 153 ± 3 pS (n = 9) and 178 ± 7 pS (n = 7) in 0 and 10 μM $[Ca^{2+}]_{in}$, respectively. The lower γ in 0 $[Ca^{2+}]_{in}$ ($P < 0.05$) may result from block by internal Mg^{2+}. A similar difference ($P < 0.01$) was obtained with 5 mM K^+ outside and 140 mM inside in the inside-out (IO) configuration with 100 nM $[Ca^{2+}]_{in}$; calculated γ values were 149 ± 3 pS (n = 10) and 167 ± 3 pS (n = 15) with 2 mM and 0 $[Mg^{2+}]_{in}$, respectively. Under a symmetrical (140 mM) K^+ condition (IO, 0 $[Ca^{2+}]_{in}$), the single-channel conductance was appreciably greater, being 220 ± 10 pS (n = 10), and the conductance value increased further to 264 ± 7 pS (n = 11) when Mg^{2+} was removed from the internal solution.

The voltage dependence of open probability (P_{open}) was consistent with that determined from the whole-cell measurements. In 0 $[Ca^{2+}]_{in}$, $V_{0.5}$ determined from the single-channel openings was 19.7 ± 1.4 mV (OO, n = 9) and 24.9 ± 3.2 mV (IO, n = 15) and the corresponding k_a values were 10.3 ± 0.9 mV and 10.0 ± 0.8 mV. In 10 μM $[Ca^{2+}]_{in}$, the channels were fully activated at −40 mV and a small decrease in P_{open} was observed at positive voltages. The open probability strongly depended on $[Ca^{2+}]_{in}$ (Fig. 2*C*). The Ca^{2+} dependence of the open probability at −20 mV (Fig. 2*D*) showed that the half-maximal activation concentration (EC_{50}) was 437 ± 266 nM with a Hill coefficent of 2.2 ± 0.7 (n = 5). The close similarity of the single-channel and whole-cell results strongly supports the notion that a BK_{Ca}-like channel type predominates the LNCaP whole-cell conductance.

The high activity of this channel at physiological voltages (< 0 mV) in 0 $[Ca^{2+}]_{in}$ is surprising. Such channel activity could potentially arise either from close colocalization with Ca^{2+} channels (Marrion & Tavalin, 1998), spontaneous Ca^{2+} release from calcium stores still present in excised patches, or enhanced Mg^{2+}-activation of the channels. The results from the following experiments exclude these possibilities. Even in the virtual absence of both Ca^{2+} and Mg^{2+} on both sides of the membrane chelated with a high concentration of EGTA (10 mM) with no added divalent ions, the channels remained active. The $V_{0.5}$ and k_a values determined from (IO) single-channel measurements were 22.8 ± 8.1 mV and 10.2 ± 0.5 mV (n = 6) and those measured from whole-cell currents were 52.9 ± 1.4 mV and 16.0 ± 0.7 mV, respectively (n = 10). The measured $V_{0.5}$ value is ~100 mV left-shifted compared with that of heterologously expressed Slo1 channels under a similar condition (Horrigan et al., 1999; Meera et al., 1996). Depletion of intracellular calcium stores (Gutiérrez et al., 1999) via preincubation of LNCaP cells with thapsigargin (2 h, 0.5 μM) had no effect on the $V_{0.5}$ and k_a values (28.8 ± 8.2 mV and 12.5 ± 1.7 mV, respectively, n = 5). Addition of 2 mM Mg^{2+} to the cytoplasmic side in the inside-out configuration only slightly

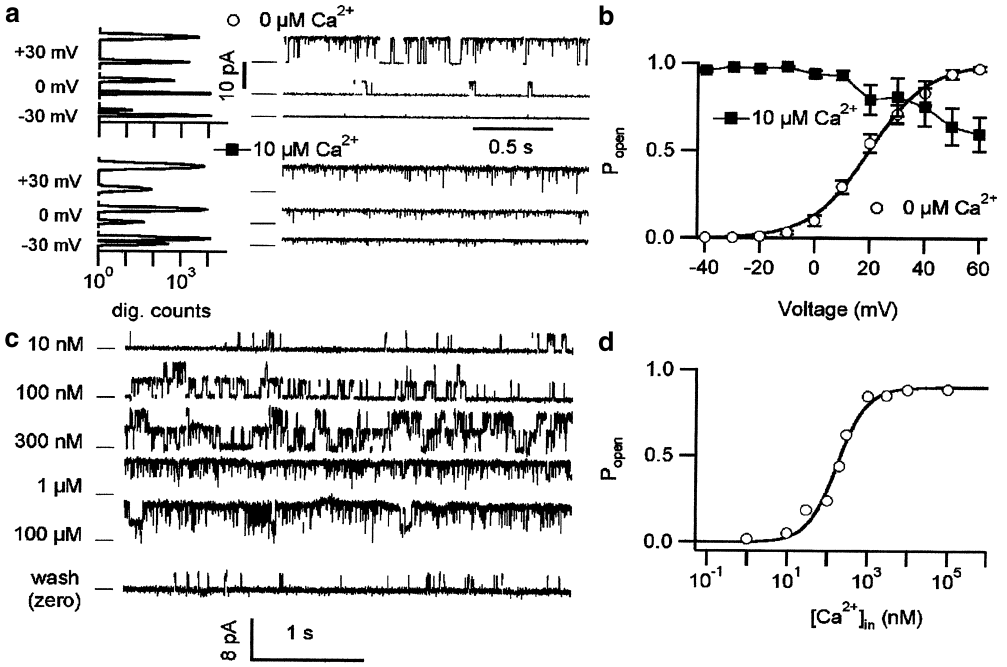

Fig. 2. Single-channel analysis of LNCaP K^+ channels. (*A*) Representative current recordings from outside-out patches containing single channels with 0 (*top*) and 10 μM (*bottom*) $[Ca^{2+}]_{in}$. Bars on the left indicate the current level of the closed channels. Note that channels open in a voltage-dependent manner in 0 $[Ca^{2+}]$, while they are mostly in an open state in 10 μM Ca^{2+}. Corresponding all-points amplitude histograms, placed on the left to the current traces, were fitted with double Gaussian functions (lines). (*B*) comparison of mean open probabilities (P_{open}) as a function of voltage in 0 (*circles*) and 10 μM free Ca^{2+} (*squares*). Mean data for 0 Ca^{2+} were fitted with Eq. 1 yielding $V_{0.5}$ of 19.9 mV and k_a of 10.6 mV, indistinguishable from averages of individual fits (*see* text). (*C*) Current recordings at −20 mV from an inside-out patch containing two channels at the indicated Ca^{2+} concentrations. (*D*) Corresponding Ca^{2+} dependence of P_{open}, determined from 2-min recordings for each Ca^{2+} concentration. Data were fitted with Eq. 4 (*line*) yielding an EC_{50} of 204 nM and a Hill coefficient of 1.6.

left-shifted $V_{0.5}$ to 10.2 ± 3.8 mV ($P < 0.05$) without affecting k_a (8.5 ± 1.0 mV, $P > 0.05$, $n = 4$). The results presented thus far show that LNCaP cells express a voltage- and Ca^{2+}-dependent, high-conductance K^+ channel with a markedly left-shifted $V_{0.5}$. Hereafter we refer to this channel as a BK_L channel.

Modulation of BK_L Channels in LNCaP Cells

The high BK_L activity at low voltages and 0 $[Ca^{2+}]_{in}$ is unprecedented, but smaller left-shifts in $V_{0.5}$ of hSlo1 / BK_{Ca} channels by BK_{Ca}-specific activators, methionine oxidation, phosphorylation, and high concentrations of cytoplasmic Mg^{2+} have been reported (Weiger et al., 2002). Therefore, we tested whether these treatments were less effective in BK_L channels than in hSlo1 / BK_{Ca} channels. NS1619 at 50 μM and 100 μM robustly activated BK_L channels in LNCaP cells (0 $[Ca^{2+}]_{in}$ Fig. 3*A*) and shifted the whole-cell $V_{0.5}$ by −60.4 ± 1.9 mV ($n = 5$) and −70.4 ± 4.2 mV ($n = 3$) respectively, which are similar to what has been reported for Slo1 channels (Dworetzky et al., 1996; Strøbaek et al., 1996).

Oxidation of three specific methionine residues in the cytoplasmic domain promoted by the oxidant chloramine-T (Ch-T) increases the activity of hSlo1 / BK_{Ca} channels (Santarelli et al., 2004; Santarelli et al., 2006). A 1-min exposure of LNCaP cells to Ch-T (1 mM) markedly facilitated whole-cell BK_L activation by shifting $V_{0.5}$ by −28.6 ± 3.0 mV ($n = 4$) (0 $[Ca^{2+}]_{in}$ Fig. 3*B*). This shift in $V_{0.5}$ is similar to that observed in the hSlo1 channel (Santarelli et al., 2004).

ATP has been reported to enhance the BK_{Ca} channel activity (Schubert & Nelson, 2001). Inclusion of MgATP (2 mM) in the presence of 100 nM Ca^{2+} in the internal solution shifted the whole-cell $V_{0.5}$ value from 32.1 ± 1.1 mV ($n = 32$) to 12.8 ± 1.7 mV ($n = 32$; $P < 0.001$). This shift in $V_{0.5}$ likely resulted from the direct action of Mg^{2+} because Mg^{2+} alone (2 mM) had a similar effect.

Cytoplasmic Mg^{2+} exerts two distinct effects on the Slo1 channel; Mg^{2+} blocks the channel pore in an apparently voltage-dependent manner but also activates the channel (Shi & Cui, 2001). Internal Mg^{2+} (100 mM) strongly blocked the BK_L outward current at +100 mV (Fig. 3*C left*) but dramatically shifted the voltage dependence to the negative direction (Fig. 3*C right*). The mean $\Delta V_{0.5}$ value was −94.5 ± 5 mV ($n = 6$) similar to what has been reported for mSlo1 channels (Shi & Cui, 2001).

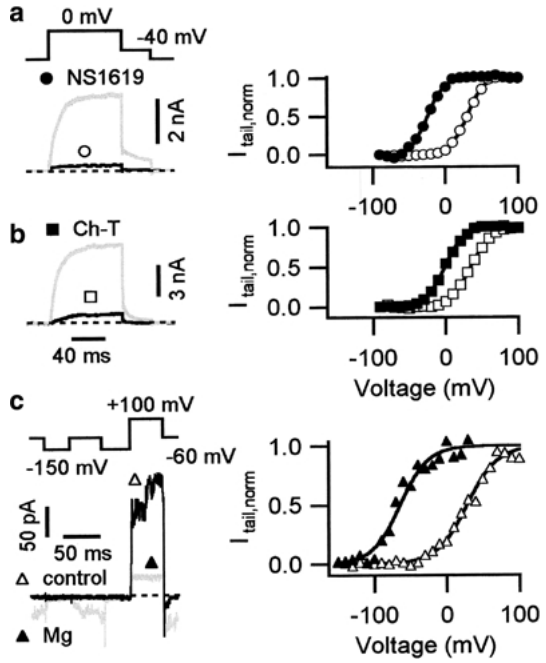

Fig. 3. BK_{Ca}-specific modulation of BK_L channels in LNCaP cells. (*A, B*) LNCaP whole-cell currents with 0 $[Ca^{2+}]_{in}$ and 5 mM external K^+ before and after addition of 50 μM NS1619 and 1-min perfusion with 1 mM chloramine-T (*Ch-T*), respectively. Corresponding normalized tail currrent ($I_{tail,norm}$)/voltage curves are shown on the right. (*C*) The effect of intracellular $[Mg^{2+}]$ was analyzed in inside-out patches from LNCaP cells in 140 mM external K^+. In 100 mM Mg^{2+}, BK_L channels are partially activated at −60 mV, deactivate at −150 mV and permit outward current at +100 mV, clearly reduced, compared to control (0 Mg^{2+}). Corresponding $I_{tail,norm}$/voltage curves are shown on the right.

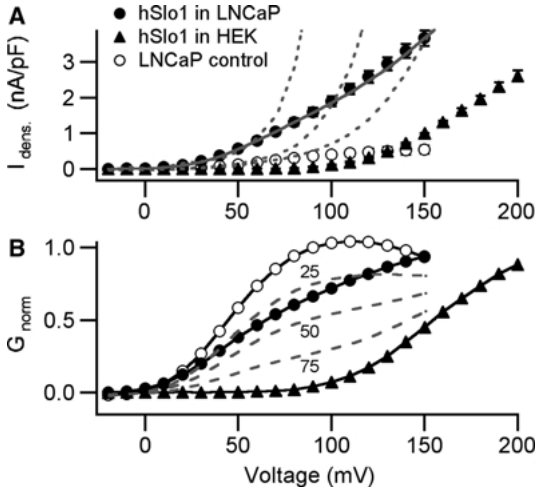

Fig. 4. Transient expression of *hSlo1* in LNCaP cells. (*A*) Mean whole-cell current densities of EGFP (*empty circles*) and *hSlo1* (*filled circles*) transfected LNCaP (Slo-LNCaP) cells upon 100-ms depolarizations. hSlo1 current densities (*triangles*), obtained from inside-out recordings of *hSlo1*-expressing HEK293 cells, were scaled to fit the slope conductance of Slo-LNCaP. The dashed lines represent attempts to fit the Slo-LNCaP conductance with the sums of control LNCaP conductance plus multiples of hSlo1 conductance as obtained in HEK293 cells to fit the mean current-density at +50, +100, and +150 mV, respectively. The solid line resembles the sum of the 4.2-fold endogenous LNCaP currents plus multiples of hSlo1 currents. Corresponding G_{norm}/voltage plots (*B*) clearly show that hSlo1 channels seem to be transformed to the BK_L-phenotype upon expression in LNCaP cells. Linear summations of BK_L and hSlo1 G_{norm}/V data are shown as dashed lines. Numbers indicate the percentage contribution of hSlo1. Error bars are left out for clarity.

Direct Involvement of hSlo1 in LNCaP Conductance

The close similarity between the Slo1 and BK_L channels in their responses to the multiple modulators suggests that the left-shift in voltage dependence of BK_L channels is caused by different means, maybe novel hSlo1 isoforms that contribute to the BK_L channel. Alternatively, we reasoned that some factor(s) unique to LNCaP cells may modify the properties of standard hSlo1 channels to give rise to the BK_L channels. Thus we heterologously expressed hSlo1 in LNCaP cells to see if the resulting currents resemble the endogenous BK_L currents. Consistent with previous reports (Meera et al., 1996; Horrigan et al., 1999), marked activation of the hSlo1 channels expressed in HEK293 cells with 0 μM $[Ca^{2+}]_{in}$ required large depolarization; the mean $V_{0.5}$ value was 155 ± 4 mV and the slope factor (k_a) was 19.9 ± 0.9 mV (n = 10). Transfection of LNCaP cells with the same hSlo1 construct increased the whole-cell current density at +100 mV by a four-fold compared with the control LNCaP cells transfected with EGFP. Furthermore, the voltage dependence of the whole-cell current densities in the LNCaP cells transfected with hSlo1 was not adequately described by linear summations of the voltage dependence of the endogenous BK_L currents in the control LNCaP cells and multiples of the hSlo1 currents in HEK293 cells (Fig. 4*A*). The G_{norm} / V relation of the currents in the LNCaP cells transfected with hSlo1 more closely resembled that of BK_L channels and was very different from that of hSlo1 expressed in HEK293 cells (Fig. 4*B*). Simple linear summations of the hSlo1 G_{norm} / V curve obtained in HEK293 cells and the G_{norm} / V curve of the endogenous BK_L channel in a ratio of 1:3 roughly describe the voltage dependence of the currents recorded in the LNCaP cells transfected with hSlo1 (Fig. 4*B*). The results thus support the idea that expression of hSlo1 in LNCaP cells leads to expression of a novel K^+ channel whose voltage dependence is markedly different from the hSlo1 channel expressed in HEK293 cells.

If cytosolic proteins expressed in LNCaP cells but not in HEK293 cells confer the unusual voltage dependence to the hSlo1 channel, acute application of cell extracts from LNCaP may modify the properties of hSlo1 channels in HEK293 cells so that the

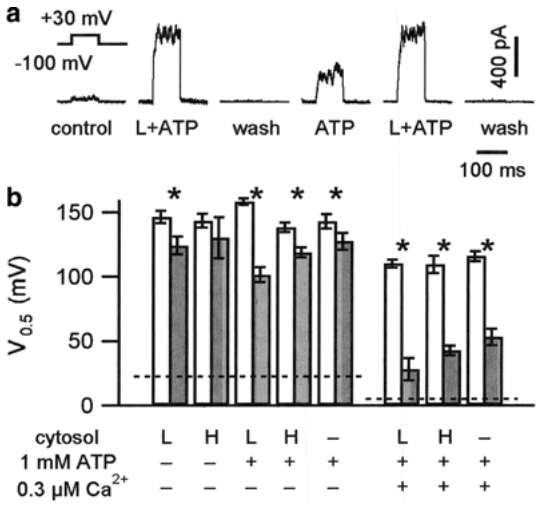

Fig. 5. Modulation of hSlo1 channels by cell lysates. (*A, B*) Effect of cytosolic LNCaP (*L*) or HEK2g3 (*H*) cell extracts on hSlo1 channels expressed in HEK293 cells. (*A*) Representative current responses to +30 mV depolarizations in 0.3 μM Ca^{2+} following superfusion of the patches with LNCaP cytosolic extracts and ATP. Corresponding *I*/*V* data, with and without Ca^{2+} (0.3 μM) and ATP (1 mM), for LNCaP (*L*) and HEK293 (*H*) cytosolic extracts, were fitted with Eq. (2) resulting in $V_{0.5}$ data shown in (*B*), averaged for 4–6 patches, each. Open bars show control $V_{0.5}$ data before superfusion of the patches with solutions containing ATP and/or cytosolic extracts, as indicated, resulting in $V_{0.5}$ data represented by the shaded bars. The dashed lines indicate the $V_{0.5}$ for BK_L channels under the respective control conditions (left group 0 Ca^{2+}, right group 0.3 μM Ca^{2+}). *: $P < 0.05$.

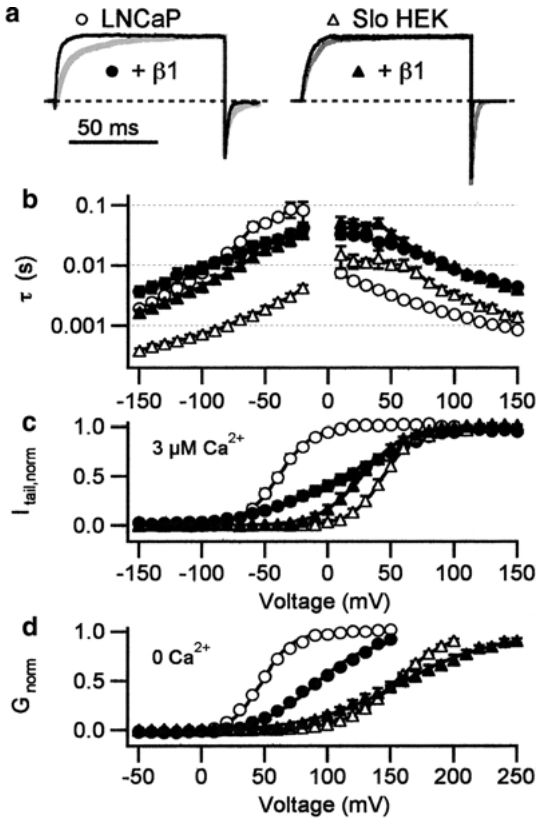

Fig. 6. Expression of *hSlo-β1* affects BK_L conductance in LNCaP cells. (*A*) Activation (+100 mV) and deactivation (−150 mV) kinetics of whole-cell LNCaP currents (*left*) and inside-out hSlo1 currents (HEK293) (*right*) with and without *hSlo-β1* expression. Currents, measured with 3 μM free Ca^{2+} in 140 mM K^+, were normalized to their steady-state outward current. (*B*) The current time course was fitted with monoexponential functions, yielding time constants, averaged among 9–15 cells/patches and plotted against voltage. (*C*) Normalized tail-current amplitudes ($I_{tail,norm}$) at −100 mV following 250-ms depolarizations to different voltages, averaged and plotted against voltage. (*D*) G_{norm} data calculated from steady-state outward currents (Eq. 2) measured in 0 μM $[Ca^{2+}]_{in}$ with 5 mM K^+ outside. Lines in (*C*) and (*D*) resemble best fits with Boltzmann functions, with $V_{0.5}$ and k_a data given in the text. Note the difference in axis range of panels *C* and *D*.

channels resemble endogenous BK_L channels in LNCaP cells. Crude cell extracts were prepared by 10-times passaging through a 26-G needle and separated from the insoluble fraction by centrifugation. Application of the LNCaP extract together with MgATP (1 mM) to the cytoplasmic side of inside-out patches taken from hSlo1–expressing HEK293 cells increased the peak current size at +30 mV by 40-fold (Fig. 5*A*), much greater than the effect of MgATP alone ($P < 0.05$). This current-enhancing effect of the cell extract and MgATP involved a shift in the voltage dependence of the hSlo1 channel to the negative direction (Fig. 5*B*). When applied in 0 $[Ca^{2+}]_{in}$, the extracts from HEK293 and LNCaP cells shifted the hSlo1 $V_{0.5}$ value by −20 mV, similar to that observed with MgATP (1 mM). In the presence of MgATP (1 mM) and 0 $[Ca^{2+}]_{in}$, the LNCaP extract produced a greater ($P < 0.05$) shift in $V_{0.5}$ than the HEK293 extract did. With 0.3 μM $[Ca^{2+}]_{in}$, the $V_{0.5}$ shifts by both extracts were greater (up to −80 mV with LNCaP extract, *see* Fig. 5*B*). Similar left-shifts were observed for BK_L channels themselves exposed to the LNCaP extract with MgATP (*not shown*). The $V_{0.5}$ shifts were always reversible with wash. The $\Delta V_{0.5}$ values were too small to fully account for the BK_L phenotype. In addition, BK_L channels in inside-out patches showed no rundown, as expected when bound proteins dissociate. Even application of 0.01–0.1% Triton X-100 to LNCaP inside-out patches did not reduce BK_L activity. In fact, Triton X-100 led to a further left-shift of $V_{0.5}$ (*not shown*). Therefore, endogenous cytosolic proteins do not underlie the modification of hSlo1 channels in LNCaP cells.

Effect of *hSlo-β1* Expression on LNCaP Conductance

To test whether association of hSlo1 α subunits with a novel β subunit (β_L) underlies the BK_L phenotype, we overexpressed hSlo-β1 to displace these putative endogenous β_L subunits. As shown in Fig. 6, hSlo1-β1 slowed down hSlo1 activation (~3-fold) and deacti-

vation (~7-fold) and left-shifted hSlo1 $V_{0.5}$ in HEK293 cells. When expressed in LNCaP cells, hSlo-β1 slowed down the whole-cell activation kinetics prominently (~6-fold) and slightly (< 2-fold) affected the deactivation kinetics in a voltage-dependent manner at 3 μM $[Ca^{2+}]_{in}$ (Fig. 6*A, B*). The voltage dependence was also noticeably affected, such that the I_{tail} / V relation of the whole-cell currents lay between those of the BK_L channels in LNCaP cells and hSlo1 channels expressed in HEK293 cells (Fig. 6*C*). The $V_{0.5}$ value of the whole-cell currents in the LNCaP cells transfected with hSlo-β1 was 14.1 ± 5.9 mV (n = 14) and the k_a value was 33.2 ± 2.3 mV. In contrast, for BK_L, hSlo1 in HEK293 cells, and hSlo1 + hSlo-β1 in HEK293 cells, the estimated $V_{0.5}$ values were −38.6 ± 2.7 (n = 15), 44.3 ± 2.9 (n = 11), and 26.9 ± 3.6 mV (n = 9), respectively, and the corresponding k_a values were 12.1 ± 0.5, 12.2 ± 1.0, and 15.6 ± 0.5 mV.

While inducing a left-shift of $V_{0.5}$ in the presence of micromolar calcium, in the absence of Ca^{2+}, the β1 subunit does not markedly alter the voltage dependence of (standard) hSlo1 channel (Fig. 6*C*, Meera et al., 1996). In contrast, β1 expression affects BK_L voltage dependence in 0 and 3 μM $[Ca^{2+}]_{in}$ similarly (*compare* Fig. 6*C*, and *D*).

In 0 $[Ca^{2+}]_{in}$ *hSlo-β1* transfected LNCaP cells exhibited a $V_{0.5}$ of 94.5 ± 3.1 mV (n = 20) compared to BK_L (48.1 ± 1.4 mV, n = 18), hSlo1 (152 ± 3 mV, n = 9), and hSlo1 + hSlo-β1 channels (162 ± 7 mV, n = 12) with corresponding k_a values of 25.2 ± 1.1, 13.3 ± 0.5, 21.8 ± 0.8, and 34.2 ± 2.0 mV.

These data indicate Ca^{2+}-independent interactions between overexpressed hSlo-β1 and endogenous BK_L channel subunits. Functional interaction was further proven by oxidation experiments: Treatment with Ch-T of the LNCaP cells transfected with *hSlo-β1* shifted the $V_{0.5}$ of the whole-cell currents by −52.4 ± 5.7 mV (n = 6) in the absence of Ca^{2+}. This shift is ~2-fold greater than that observed with BK_L without hSlo-β1 overexpression and is also consistent with the greater effect of oxidation reported in hSlo1 led to β1 expressed in HEK293 cells (Santarelli et al., 2004).

The changes in the kinetics and the voltage dependence of the whole-cell currents in LNCaP cells by overexpression of hSlo-β1 described above are similar to the reported effects of β1 in other expression systems (Santarelli et al., 2004). Thus, the observed changes in LNCaP cells are likely to result from the functional interactions between hSlo-β1 and BK_L proteins. However, the (right) shift of $V_{0.5}$ of LNCaP whole-cell currents upon hSlo-β1 expression is contrary to the (left) shift of $V_{0.5}$ upon hSlo-β1 expression in (hSlo1 expressing) HEK293 cells. This might represent either the result of functional interactions between hSlo-β1 and novel *hSlo* variants (α_L) or the result of (partial) displacement of endogenous β_L by heterologously expressed hSlo-β1 subunits with (standard) hSlo1 α subunits, endogenous to LNCaP cells.

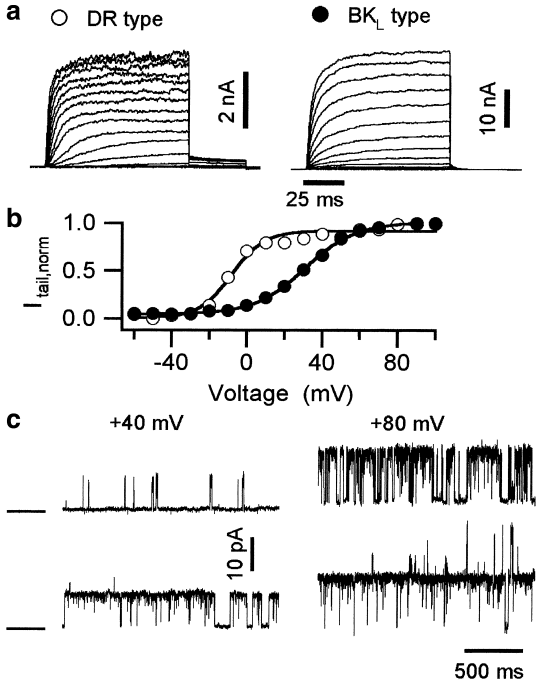

Fig. 7. BK_L-like currents in T47D breast cancer cells. (*A*) Representative whole-cell currents of two different T47D cells containing delayed rectifier (*DR*) or BK_L type voltage-dependent K^+ channels, measured under the same conditions as for Fig. 1 in 0 $[Ca^{2+}]_{in}$. Corresponding $I_{tail,norm}/V$ plots are shown in (*B*). (C) Outside-out single-channel recordings at +40 mV (*left*) and +80 mV (*right*) of two different cells containing BK_L-like channels. Bars left to the current traces indicate the closed-state current level.

BK_L-Like Channels in T47D Cells

In search for other proliferating cells expressing BK_L channels, we screened various cell lines, including melanoma (IGR1, IGR39, IPC298) and neuroblastoma (SH-SY5Y, SK-N-AS, SK-N-MC, SK-N-SH, SK-N-FI), and T47D breast cancer cell lines. Only T47D breast cancer cells showed a positive signal for hSlo1 transcription using RT-PCR and were further analyzed with the patch-clamp technique. The ionic currents in T47D cells exhibited at least two components (Fig. 7*A*). The first was classified as a delayed-rectifier (DR) type K^+ channel, since it was voltage dependent, outwardly rectifying, non-inactivating, and K^+-selective (V_{rev} < −40mV). A second outward K^+ current, present in < 5% of the cells, clearly differed in voltage dependence (Fig. 7*B*). Outside-out patch-clamp recordings (Fig. 7*C*) revealed large-conductance K^+ channel openings (163 ± 11 pS, n = 6), reminiscent of BK_L channels. With 2 mM $[Mg^{2+}]_{in}$ and 0 $[Ca^{2+}]_{in}$ the $V_{0.5}$ estimated from the whole-cell tail-currents was 45.6 ± 6.5 mV

(k_a = 8.5 ± 0.8 mV, n = 6) 60 mV left-shifted compared to hSlo1 ($V_{0.5}$ = 110 ± 4 mV, k_a = 17.4 ± 2.9 mV, n = 17) or hSlo1 + hSlo-β1 channels ($V_{0.5}$ = 115 ± 9 mV, k_a = 21.4 ± 1.1 mV, n = 17). We note that T47D cells contain more than one type of BK_L-like channels, clearly differing in voltage dependence (Fig. 7*C*).

Growth of T47D and LNCaP cells depends on hormones, progesterone and androgens, respectively. We therefore tested whether expression or biophysical properties of BK_L channels in LNCaP cells may change under different growth conditions. We found that withdrawal of serum from the growth medium markedly slowed the LNCaP cell proliferation and changed the cell morphology from being predominantly bipolar, weakly adherent cells to multipolar, strongly adherent cells with longer, thinner, and branched processes. In addition, serum deprivation for two weeks significantly decreased the whole-cell current density at +100 mV with 0 $[Ca^{2+}]_{in}$ from 1.19 ± 0.10 nA / pF to 0.25 ± 0.02 nA / pF (n = 103, each) and reintroduction of serum to the medium recovered the density to the control level in one week (1.36 ± 0.14 nA / pF, n = 53). The reduction of current density was likely due to the absence of sex hormones and/or other lipophilic substances like growth factors. Removal of these components from the serum used for cell culture via charcoal treatment similarly decreased the current density to 30.9 ± 4.1% (n = 4 experiments, each with 35 cells per group) within 5 days. This decrease, however, did not result from the lack of androgens since the current decrease was unaffected by an antagonist (100 nM casodex) or an agonist (100 pM R1881); the current densities of casodex- or R1881-treated cells were significantly reduced (to 30.1 ± 8.3% and 30.9 ± 4.3%; n = 4 experiments, $P < 0.01$) compared with control cells, but not different from cells treated with charcoal-treated serum (CTS). The voltage dependencies of the LNCaP whole-cell currents in the control and CTS-treated cells were indistinguishable; in 0 $[Ca^{2+}]_{in}$ and 2 mM $[Mg^{2+}]_{in}$, the whole-cell $V_{0.5}$ values were 34.6 ± 1.4 mV (control) and 35.2 ± 2.4 mV (CTS). However, these $V_{0.5}$ values were significantly different ($P < 0.05$) from those obtained for the CTS + casodex (42.0 ± 1.8 mV) or CTS + R1881 (41.6 ± 1.6 mV) -treated cells (n = 35, each), We have to conclude that the BK_L phenotype, i.e., the strong left-shift in $V_{0.5}$ does not result from an androgen signal and speculate that BK_L expression is not restricted to sex hormone-dependent cells.

Discussion

K^+ Channels in LNCaP Cells

Conflicting results have been reported regarding K^+ channels in LNCaP cells. Here we show that BK_L, a BK_{Ca} channel with unusual properties, predominates large robust whole-cell currents in LNCaP cells. In contrast, Skryma et al. (1999) measured ~20-fold smaller whole-cell currents (580 pA *vs.* 12.4 nA at +40 mV) and attributed the currents to a Ca^{2+}-inhibited, 78-pS, voltage-dependent K^+ channel. We observed BK_L channels in LNCaP and T47D cells obtained from DSMZ (Germany) as well as in independently grown LNCaP cells obtained from ATCC (USA) and LNCaP-derived androgen-independent C4-2 cells (Thalmann et al., 1994; *not shown*). In the cells used by Skryma and coworkers (1999), BK_L expression may be down-regulated due to clonal selection or different culture conditions. However, the culture condition described by Skryma et al. (1999) was essentially identical to that in our study except for the reagent suppliers and the addition of antibiotics. In our hands, BK_L density was reduced neither by addition of antibiotics (1.4 ± 0.3 nA / pF, n = 25) nor by cultivation in completely different (HEK293) medium (1.0 ± 0.1 nA / pF, n = 35) within 4 weeks, suggesting that not the presence, but rather the absence of BK_L currents is the exception. We speculate that differences in the sera used for cell culture may be important. Our results exclude any regulatory role for the androgen receptor but instead favor the involvement of receptors for other steroids (e.g., estrogens or glucocorticoids) or growth factors that also are removed in the charcoal-treated serum. Expression and physiological functions of BK_L channels in prostate LNCaP precursor cells as well as the mechanism of BK_L-regulation in LNCaP cells need to be investigated in the future. These issues are important because serum starvation *increases* BK_{Ca} activity in glioma cells (Weaver et al., 2004).

Characteristics of BK_L Channels

All BK_{Ca} channels share common features: (1) High single-channel conductance in combination with strong K^+ selectivity and (2) voltage dependence that is allosterically modified (left-shift in $V_{0.5}$) by an increase in $[Ca^{2+}]_{in}$, $[Mg^{2+}]_{in}$ or by BK_{Ca}-specific activators (Kaczorowski et al., 1996; Gribkoff et al., 1997; Orio et al., 2002). The BK_L channel in LNCaP cells meets all these criteria and, hence, (per definition) is a novel type of BK_{Ca} channel. Although inhibition of BK_L channels by ChTx, IbTx, paxilline, and penitrem A is slightly less potent compared with hSlo1 / BK_{Ca} channels (Knaus et al., 1994; Dworetzky et al., 1996; Strøbaek et al., 1996; Meera et al., 2000; Lippiat et al., 2003), the rank order of potency of the blockers is the same.

BK_L clearly differs from conventional hSlo1 channels, especially in its voltage dependence; in 0 $[Ca^{2+}]_{in}$ $V_{0.5}$ of BK_L channels is around +50 mV, about 100 mV left-shifted compared with hSlo1 channels (+155 mV). Furthermore, BK_L channels exhibit an about 10-fold lower EC_{50} for

Ca^{2+}-dependent activation (440 nM at −20 mV *vs.* 4.1 μM at +50 mV for hSlo1 channels) although the Hill coefficient of the overall Ca^{2+} dependence is similar to that of hSlo1 (n = 2.2 *vs.* 2.8). Therefore, in contrast to BK_{Ca} channels, BK_L channels are expected to be noticeably activated under physiological resting conditions; ~2 mM $[Mg^{2+}]_{in}$, ~100 nM $[Ca^{2+}]_{in}$, and a resting potential of around −25 mV.

Low EC_{50} values for calcium-dependent activation of BK_{Ca} channels are not unique for LNCaP cells. They have also been reported for various cancer cell lines (Kraft et al., 2000; Basrai et al., 2002; Liu et al., 2002) and non-cancer cells (Anwer et al., 1992; Sansom & Stockand, 1994). This may result from specific Slo1 α subunits, like a glioma-BK isoform (Liu et al., 2002), or from differences in signaling pathways that also affect BK_{Ca} channels. In contrast the strong shift in $V_{0.5}$ appears specific for BK_L, which raises the question regarding expression pattern and possible physiological roles of this channel. Since we found no indication for androgen dependence of channel expression or biophysical channel features in LNCaP cells, BK_L channels may also exist in sex hormone-independent, non-cancerogenic cells/tissues. In fact, BK_L-like currents might have been overlooked, i.e., taken for K_v channels, due to their high activity in 0 $[Ca^{2+}]_{in}$. A BK_{Ca} channel with a similar shifted voltage dependence was functionally described in inner hair cells from mouse and rat (Thurm et al., 2005). Future investigations have to clarify whether BK_L channels in LNCaP cells represent the corresponding channels in humans.

Speculations about the Molecular Basis of BK_L Channels

Those reagents and treatments that are known to left-shift the activation of BK_{Ca} channels, such as Ca^{2+}, Mg^{2+}, BK_{Ca} activators, and Ch-T mediated oxidation, also affected BK_L channels in the same manner. Although this is no direct proof, we hypothesize that these means are not the crucial factors for determination of the difference between the voltage dependencies of BK_L and hSlo1 channels. With our results we cannot firmly exclude that a novel phosphorylation pattern in LNCaP and T47D cells cause the BK_L phenotype. The observed reversibility of ATP effects and the stability of channel activity upon patch excision in ATP-free solution indicate that, if at all, lack of dephosphorylation is important in this respect. Up to date, however, a 100-mV left-shift has been described neither due to dissociation of phosphatases nor due to drug-mediated inhibition of phosphatases (Schubert & Nelson, 2001). Cytoplasmic proteins are unlikely to be responsible for the BK_L phenotype either. For BK_L channels, we neither observed washout of putative cytoplasmic proteins, nor could intracellular application of cytosolic extracts from LNCaP cells transform hSlo1 channels to the BK_L phenotype (Fig. 5).

BK_{Ca} channels are multimeric complexes formed by four Slo1 α subunits that can coassemble with up to four accessory β subunits (Orio et al., 2002). Several Slo1 α subunit splice variants and different β subunits provide a huge number of possible combinations. Even point mutations or polymorphisms in both, Slo1 α (Díaz et al., 1998; Lippiat et al., 2000) and Slo-β1 (Fernández-Fernández et al., 2004), can result in tremendous functional changes. The diversity is further increased by the variable stoichiometry of Slo1 α and β subunits (Wang et al., 2002) and posttranslational modifications like phosphorylation (Zhou et al., 2001; Erxleben et al., 2002), which in turn can determine the effect of β subunit association (Jin et al., 2002). Because of the tremendous diversity, we cannot completely exclude that a combination of already known α and β subunits forms BK_L channels. Nevertheless, we propose that the features of BK_L channels result from a unique subunit composition including novel hSlo subunits of the α (α_L) and/or β (β_L) type, expressed in LNCaP and T47D cells.

From our transfection experiments (Fig. 4, Fig. 6), we infer that hSlo1 α and β1 subunits can participate in BK_L formation. hSlo-β1 expression in LNCaP cells clearly affects BK_L whole-cell current kinetics and voltage dependence without effect on current density. In addition, the increased susceptibility to Ch-T (Santarelli et al., 2004) clearly indicates functional interaction. Assuming that α_L subunits are responsible for the BK_L phenotype, LNCaP cells represent an interesting system to study the molecular mechanism of α / β interactions in BK_{Ca} channels since the functional effects of hSlo-β1 on α_L (calcium-independent right-shift of $V_{0.5}$) would be in part contrary to those on standard α subunits (calcium-dependent left-shift of $V_{0.5}$). On the other hand, the effects of hSlo-β1 expression may be also explained by functional replacement of β_L subunits and their main functional effect, i.e., the Ca^{2+}-independently left-shifted $V_{0.5}$. Both scenarios would be compatible with the 4-fold increase in BK_L density observed upon hSlo1 expression in LNCaP cells assuming that one α_L and/or β_L subunit is sufficient to transform BK_{Ca} to BK_L channels.

Future studies will have to identify the molecular counterparts of the BK_L phenotype which may give further insight into Slo α / β subunit interaction as well as the synergistic channel activation by voltage and calcium.

We are grateful for technical assistance by S. Arend and A. Rossner and for helpful discussions with R. Schönherr. This work was supported by the DFG (HE 2993/2), TMWFK (B378-01027) and National Institute of Health.

References

Anwer, K., Toro, L., Oberti, C., Stefani, E., Sanborn, B. M. 1992. Ca^{2+}-activated K^+ channels in pregnant rat myometrium: modulation by a β-adrenergic agent. *Am. J. Physiol.* **263:**1049–1056

Basrai, D., Kraft, R., Bollensdorff, C., Liebmann, L., Benndorf, K., Patt, S. 2002. BK channel blockers inhibit potassium-induced proliferation of human astrocytoma cells. *Neuro Report* **13:**403–407

Brenner, R., Perez, G.J., Bonev, A.D., Eckman, D.M., Kosek, J.C, Wiler, S.W., Patterson, A.J., Nelson, M.T., Aldrich, R.W. 2000. Vasoregulation by the β1 subunit of the calcium-activated potassium channel. *Nature* **407:**870–876

Dıaz, L., Meera, P., Amigo, J., Stefani, E., Alvarez, O., Toro, L., Latorre, R. 1998. Role of the S4 segment in a voltage-dependent calcium-sensitive potassium (hSlo) channel. *J. Biol. Chem.* **273:**32430–32436

Dworetzky, S.I., Boissard, C.G., Lum-Ragan, J.T., McKay, M.C., Post-Munson, D.J., Trojnacki., J.T., Chang, C.-P., Gribkoff, V.K. 1996. Phenotypic alteration of a human BK (hSlo) channel by hSloβ subunit coexpression; changes in blocker sensitivity, activation/relaxation and inactivation kinetics, and protein kinase A modulation. *J. Neurosci.* **16:**4543–4550

Erxleben, C., Everhart, A.L., Romeo, C., Florence, H., Bauer, M.B., Alcorta, D. A., Rossie, S., Shipston, M.J., Armstrong, D.L. 2002. Interacting effects of N-terminal variation and strex exon splicing on slo potassium channel regulation by calcium, phosphorylation, and oxidation. *J. Biol. Chem.* **277:**27045–27052

Fernández-Fernández, J.M., Tomás, M., Vázquez, E., Orio, P., Latorre, R., Senti, M., Marrugat, J., Valverde, M.A. 2004. Gain-of-function mutation in the KCNMB1 potassium channel subunit is associated with low prevalence of diastolic hypertension. *J. Clin. Invest.* **113:**1032–1039

Gribkoff, V.K., Starret, J.E. Jr., Dworetzky, S.I. 1997. The pharmacology and molecular biology of large-conductance calcium-activated (BK) potassium channels. *Adv. Pharmacol.* **37:**319–348

Gutiérrez, A.A., Arias, J.M., Garcia, L., Mas-Oliva, J., Guerrero-Hernandéz, A. 1999. Activation of a Ca^{2+}-permeable cation channel by two different inducers of apoptosis in a human prostatic cancer cell line. *J. Physiol.* **517:**95–107

Horoszewicz, J.S., Leong, S.S, Kawinski, E., Karr, J.P., Rosenthal, H., Chu, T.M., Mirand, E.A., Murphy, G.P. 1983. LNCaP model of human prostatic carcinoma. *Cancer Res* **43:**1908–1918

Horrigan, F.T., Cui, J., Aldrich, R.W. 1999. Allosteric voltage gating of potassium channels I: mSlo ionic currents in the absence of Ca^{2+}. *J. Gen. Physiol.* **114:**277–304

Jin, P., Weiger, T.M., Wu, Y., Levitan, I.B. 2002. Phosphorylation-dependent functional coupling of hSlo calcium-dependent potassium channel and its hβ4 subunit. *J. Biol. Chem.* **277:**10014–10020

Kaczorowski, G.J., Knaus, H.-G., Leonard, R.J., McManus, O.B., Garcia, M.L. 1996. High-conductance calcium-activated potassium channels: structure, pharmacology, and function. *J Bioenerg. Biomembr.* **28:**255–267

Knaus, H.-G., McManus, O.B., Lee, S.H., Schmalhofer, W.A., Garcia-Calvo, M., Helms, L.M.H., Sanchez, M., Giangiacomo, K., Reuben, J.P., Smith, A.B. 3rd, Kaczorowski, G.J., Garcia, M.L. 1994. Tremorgenic indole alkaloids potently inhibit smooth muscle high-conductance calcium-activated potassium channels. *Biochemistry* **33:**5819–5828

Kraft, R., Benndorf, K., Patt, S. 2000. Large conductance Ca^{2+} activated K^+ channels in human meningioma cells. *J. Membrane Biol.* **175:**25–33

Lai, G.-J., McCobb, D.P. 2002. Opposing actions of adrenal androgens and glucocorticoids on alternative splicing of Slo potassium channels in bovine chromaffin cells. *Proc. Natl. Acad. Sci. USA* **99:**7722–7727

Lippiat, J.D., Standen, N.B., Davies., N.W. 2000. A residue in the intracellular vestibule of the pore is critical for gating and permeation in Ca^{2+}-activated K^+ (BK_{Ca}) channels. *J. Physiol.* **529:**131–138

Lippiat, J.D., Standen, N.B., Harrow, I.D., Phillips, S.C., Davies, N.W. 2003. Properties of BK_{Ca} channels formed by bicistronic expression of hSlo α and β1-4 subunits in HEK293 cells. *J. Membrane Biol.* **192:**141–148

Liu, X., Chang, Y., Reinhart, P. H., Sontheimer, H. 2002. Cloning and characterization of glioma BK, a novel BK channel isoform highly expressed in human glioma cells. *J. Neurosci.* **22:**1840–1849

Marrion, N. V., Tavalin, S.J. 1998. Selective activation of Ca^{2+}-activated K^+ channels by co-localized Ca^{2+} channels in hippocampal neurons. *Nature* **395:**900–905

Meera, P., Wallner, M., Toro, L. 2000. A neuronal β subunit (hKCNMB4) makes the large conductance, voltage- and Ca^{2+}-activated K^+ channel resistant to charybdotoxin and iberiotoxin. *Proc. Natl. Acad. Sci. USA.* **97:**5562–5567

Meera, P., Wallner, M., Jiang, Z., Toro, L. 1996. A calcium switch for the functional coupling between α (hslo) and β subunits ($K_{V,Ca}$β) of maxi K channels. *FEBS Lett.* **382:**84–38

Meera, P., Wallner, M., Song, M., Toro, L. 1997. Large conductance voltage- and calcium-dependent K^+ channel, a distinct member of voltage-dependent ion channels with seven N-terminal transmembrane segments (S0-S6), an extracellular N terminus, and an intracellular (S9-S10) C terminus. *Proc. Natl. Acad. Sci. USA* **94:**14066–14071

Orio, P., Rojas, P., Ferreira, G., Latorre, R. 2002. New disguises for an old channel. MaxiK channel β-subunits. *News Physiol. Sci.* **17:**156–161

Ramanathan, K., Michael, T.H., Jiang, G.-J., Hiel, H., Fuchs, P.A. 1999. A molecular mechanism for electrical tuning of cochlear hair cells. *Science* **283:**215–217

Sansom, S.C., Stockand, J.D. 1994. Differential Ca^{2+} sensitivities of BK(Ca) isochannels in bovine mesenteric vascular smooth muscle. *Am. J. Physiol.* **266:**1182–1189

Santarelli, L.C., Chen, J., Heinemann, S.H., Hoshi, T. 2004. The β1 subunit enhances oxidative regulation of large-conductance calcium-activated K^+ channels. *J. Gen. Physiol.* **124:**357–370

Santarelli, L.C., Wassef, R., Heinemann, S.H., Hoshi, I. 2006. Three methionine residues located within the regulator of conductance for K^+ (RCK) domains confer oxidative sensitivity to large-conductance Ca^{2+}- activated K^+ channels. *J. Physiol.* **571:**329–359

Schubert, R., Nelson, M.T. 2001. Protein kinases: tuners of the BK_{Ca} channel in smooth muscle. *Trends Pharmacol. Sci.* **22:**505–512

Shao, L.-R., Halvorsrud, R., Borg-Graham, L., Storm, J.F. 1999. The role of BK-type Ca^{2+}-dependent K^+ channels in spike broadening during repetitive firing in rat hippocampal pyramidal cells. *J. Physiol.* **521:**135–146

Shen, K.-Z., Lagrutta, A., Davies, N., Standen, N., Adliman, J., North, R. 1994. Tetraethylammonium block of Slowpoke calcium-activated potassium channels expressed in Xenopus oocytes: evidence for tetrameric channel formation. *Pfluegers Arch.* **426:**440–445

Shi, J., Cui, J. 2001. Intracellular Mg^{2+} enhances the function of BK-type Ca^{2+}-activated K^+ channels. *J. Gen. Physiol.* **118:**589–605

Skryma, R., van Coppenolle, P., Dufy-Barbe, L., Dufy, B., Prevarskaya, N. 1999. Characterization of Ca^{2+}-inhibited potassium channels in the LNCaP human prostate cancer cell line. *Receptors Channels* **6:**241–253

Strøbaek, D., Christopherson, P., Holm, N.R., Moldt, P., Ahring, P.K., Johansen, T.E., Olesen, S.-P. 1996. Modulation of the Ca^{2+}-dependent K^+ channel hslo, by the substituted diphenylurea NS 1608, paxilline and internal Ca^{2+}. *Neuropharmacology* **35:**903–914

Thalmann., G.N., Anezinis, P.E., Chang, S.M., Zhau, H.E., Kim, E.E., Hopwood, V.L., Pathak, S., von Eschenbach, A.C., Chung, L.W 1994. Androgen-independent cancer progression and bone metastasis in the LNCaP model of human prostate cancer. *Cancer Res*. **54:**2577–2581

Thurm, H., Fakler, B., Oliver, D. 2005. Ca^{2+}-independent activation of BK_{Ca} channels at negative potentials in mammalian inner hair cells J. *Physiol*. **569:**137–151

Tseng-Crank, J., Foster, C.D., Krause, J.D., Mertz, R., Godinot, N., DiChiara, T.J., Reinhart, P.H. 1994. Cloning, expression, and distribution of functionally distinct Ca^{2+}-activated K^+ channel isoforms from: human brain. *Neuron* **13:**1315–1330

Wang, Y.-W., Ding, J.P., Xia, X.-M., Lingie, C.J. 2002. Consequences of the stoichiometry of Slo1 α and auxiliary β subunits on functional properties of large-conductance Ca^{2+}-activated K^+ channels. *J. Neurosci*. **22:**1550–1561

Weiger, T.M., Hermann, A., Levitan, I.B. 2002. Modulation of calcium-activated potassium channels. *J. Comp. Physiol. A*. **188:**79–87

Weaver, A.K., Liu, X., Sontheimer, H. 2004. Role for calcium-activated potassium channels (BK) in growth control of human malignant glioma cells. *J. Neurosci. Res*. **78:**224–234

Xia, X.-M., Zeng, X., Lingle., C.J. 2002. Multiple regulatory sites in large-conductance calcium-activated potassium channels. *Nature* **418:**880–884

Xie, J., McCobb, D.P. 1998. Control of alternative splicing of potassium channels by stress hormones. *Science* **280:**443–446

Zhau, H.Y., Chang, S.M., Chen, B.Q., Wang, Y., Zhang, H., Kao, C., Sang, Q.A., Pathak, S.J., Chung, L.W. 1996. Androgen-repressed phenotype in human prostate cancer. *Proc. Natl. Acad. Sci. USA* **93:**15152–15157

Zhou, X.-B., Arntz, C., Kamm, S., Motejlek, K., Sausbier, U., Wang, G.-X., Ruth, P., Korth, M. 2001. A molecular switch for specific stimulation of the BK_{Ca} channel by cGMP and cAMP kinase. *J. Biol. Chem*. **276:**43239–43245